Measurement of the positron work functions of polycrystalline Fe, Mo, Ni, Pt, Ti, and V

Mohammed Jibaly
Department of Physics, University of Northern Iowa, Cedar Falls, Iowa 50614-0150

Alex Weiss, A. R. Koymen, D. Mehl,* L. Stiborek,† and C. Lei
Department of Physics, The University of Texas at Arlington, Arlington, Texas 76019
(Received 30 May 1991; revised manuscript received 23 October 1991)

We report measurements of the positron work functions ϕ^+ of polycrystalline samples of Fe, Mo, Ni, Pt, Ti, and V. The positron work functions were obtained by measuring the energy spectrum of slow positrons reemitted by the metal surfaces when bombarded with keV-energy positrons. Two methods were used to extract the work functions. The first method provides an absolute measurement. The second method infers the positron work function from measurements of $\Sigma=\mu^+ +\mu^-$ (where μ^+ and μ^- are the positron and electron chemical potentials, respectively) relative to the value of Σ for Cu and to the values of the electron work function for the surface. The second method (which circumvents many of the systematic problems of the first method since the values of Σ are independent of crystal face and surface contamination) gives $\phi^+_{\rm Fe}=-1.2(2)$ eV, $\phi^+_{\rm MO}=-2.2(2)$ eV, $\phi^+_{\rm Ni}=-1.2(2)$ eV, $\phi^+_{\rm Pt}=-1.8(2)$ eV, $\phi^+_{\rm V}=-0.6(2)$ eV, and $\phi^+_{\rm Ti}>0$. Our results are compared to theoretical predictions and to previous measurements.

I. INTRODUCTION

The positron work function is an intrinsic property of positron interactions with matter.[1] It is important for checking the validity of theoretical assumptions, for choosing particular materials for surface experiments such as reemitted-positron spectroscopy (RPS)[2] and positron-annihilation-induced Auger-electron spectroscopy (PAES),[3] and for developing improved positron moderators for use in low-energy positron beams.

In analogy with the electron work function ϕ^-, the positron work function ϕ^+ is defined as the minimum energy required to remove a thermalized positron from the bulk to a position, at rest, far from the sample. Following the Lang and Kohn[4] formulation of the electron work function,

$$\phi^-=\Delta\phi-\mu^- , \tag{1}$$

the positron work function ϕ^+ can be expressed as[5]

$$\phi^+=-\Delta\phi-\mu^+ , \tag{2}$$

where $\Delta\phi$ is the mean electrostatic potential across the surface dipole layer (arising from electron spill out at the surface), and μ^+ (μ^-) is the positron (electron) chemical potential of the material. Note that although the dipole term has the same magnitude for electrons and positrons, its contribution to ϕ^+ differs in sign because of the opposite charge of the positron. The chemical potential is strictly a bulk property; Hodges and Stott[5] pointed out that μ^+ can be separated into two parts:

$$\mu^+=E_0+E_{\rm corr} , \tag{3}$$

where E_0 is the zero-point energy arising from the positron-ion interaction and $E_{\rm corr}$ is the positron-electron correlation energy.

In some metals the sum of the terms indicated in Eqs. (2) and (3) yields a negative positron work function, that is, a negative affinity for positrons. A positron that is injected into such a solid at kilovolt energies has a high probability of reaching thermal equilibrium and diffusing to the surface, where it may be spontaneously emitted with a minimum kinetic energy that is equal to the magnitude of the (negative) positron work function, ϕ^+, of the material. This permits the measurement of negative positron work functions through the analysis of the energy of the reemitted positrons.[6]

A discussion of earlier theoretical and experimental work on positron work functions can be found in the reviews by Mills[6] and by Schultz and Lynn.[1] We report here measurements of the positron work functions of well-analyzed polycrystalline samples of six metals: Fe, Mo, Ni, Pt, Ti, and V. Measurements were also done on polycrystalline Cu which was used as a reference for all other metals. A comparison is made between our results and other measurements and related theoretical predictions.

II. EXPERIMENTAL

The apparatus used in this experiment has been described elsewhere,[7] and is similar to that used previously by Mills.[8] A magnetically guided monoenergetic positron beam is derived from a 35-mCi ^{22}Na positron source and a slow-positron (tungsten-foil) converter. An electrostatic accelerator makes it possible to vary the beam energy from $\sim$10 ev to $\sim$10 keV. Crossed electric and magnetic ($E\times B$) fields act as velocity selectors for the beam, both in the source and target chambers. The positron beam travels about 3 m from source to target, through an increasing axial magnetic field that serves to focus the beam

to a 2-mm diameter at the sample.

The target chamber includes an Auger spectrometer for characterizing the surface content of the sample, NaI crystals to detect annihilation γ rays and monitor the incident-beam intensity, a sputter ion gun, and a sample manipulator with a resistance heater for sample annealing. The base pressure in the target chamber was in the high 10^{-10}-torr range. A quadrupole mass spectrometer indicated that the residual gas consisted primarily of hydrogen, helium, and inert gases (argon and neon).

The physical characteristics of the polycrystalline foil samples were (nominally): 0.127-mm-thick copper, 99.99% free of metallic contaminants; 0.1-mm-thick iron, 99.9975% free of metallic contaminants; 0.127-mm-thick molybdenum, 99.97% free of metallic contaminants; 0.125-mm-thick nickel, 99% free of metallic contaminants; 0.025-mm-thick platinum, 99.95% free of metallic contaminants; 0.127-mm-thick titanium, 99% free of metallic contaminants; and 0.05-mm-thick vanadium, 99% free of metallic contaminants.

All samples were cleaned with ethanol prior to insertion into the UHV chamber, and then sputter cleaned *in situ* using argon or neon ions. The samples were first sputtered with high-energy ions (2 to 3 keV), and then with lower energy ions (0.5 keV) in an attempt to reduce the sputter damage to the surface. The copper, molybdenum, titanium, and vanadium foils were annealed *in situ* at 900 °C for 2 h, and later at about 600 °C for 4 h, and then sputtered. The iron foil was annealed at 500 °C for 1 h, and then sputtered. (The copper, iron, molybdenum, titanium, and vanadium samples were annealed prior to sputtering, but not after, due to a failure of the sample heater.) The nickel and platinum foils were annealed before and after sputtering for an average of one hour each time in the 750–800 °C. An Auger spectrum was taken immediately before and shortly after each experimental run to give an indication of surface contamination.

The energy spectrometer shown in Fig. 1 consists of a retarding field analyzer (RFA), along with a trochoidal analyzer[9] making use of crossed electric and magnetic fields, and a microchannel plate (MCP) assembly for the detection of charged particles. Work-function data was obtained by fixing the sample at a voltage V_S (typically +5 V to +20 V with respect to ground), and varying the

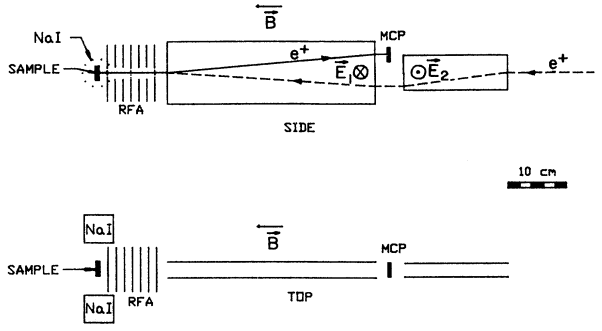

FIG. 1. A schematic diagram of the energy spectrometer. The retarding voltage is applied to the fourth of the seven stainless-steel disks which constitute the retarding field analyzer (RFA). The large and small rectangles represent the electrodes of a trochoidal analyzer which makes use of crossed electric and magnetic fields to deflect the reemitted positrons into the microchannel plate (MCP) assembly. NaI(Tl) scintillators for the detection of annihilation γ rays are mounted on either side of the sample.

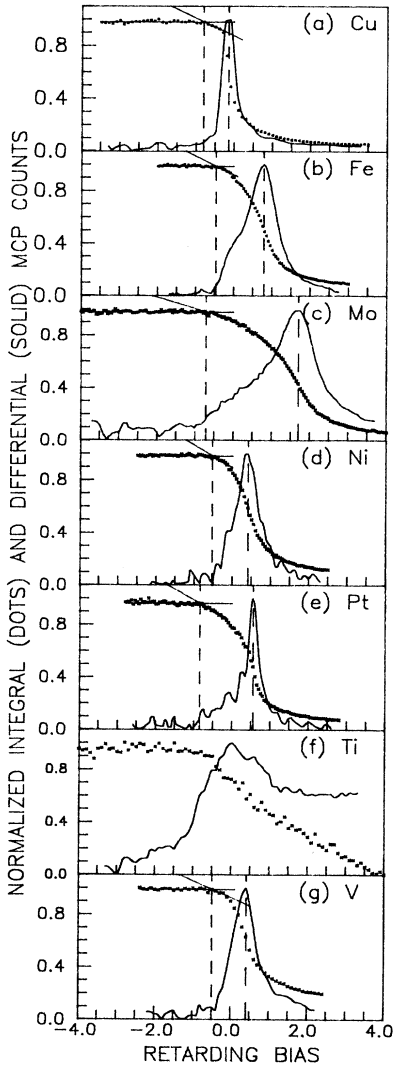

FIG. 2. Normalized integral counts (dotted curves) as a function of the retarding bias V_{RET} for (a) Cu, (b) Fe, (c) Mo, (d) Ni, (e) Pt, (f) Ti, and (g) V. The derivative of $N(V_{\mathrm{RET}})$ is also shown (solid curves). An average of the points on the high shoulder of the integral data is represented by the solid horizontal line. A least-squares fit through the first point that lies at least 3 standard deviations below the average (and includes two points on either side of this point) is indicated by the solid sloped line. The intersection of the sloped and horizontal lines is taken as the zero energy point, V_{zero}. The location of V_{zero} and steepest descent (V_{PK}) are indicated by the left and right vertical dashed lines, respectively, in each graph (except Ti). The Cu spectrum correspond to the Cu sample which was mounted together with the Mo, Ti, and V. Cu spectra (not provided) corresponding to the other three samples are similar but differ slightly in their reference points from the one provided here.

TABLE I. Compilation of sample and beam characteristics.

Sample	Surface contamination (at. %)	Incident e^+ energy (keV)	Target bias (V)	Positron yield (%)
Cu	4% C, 2% O	1.14	+10	1.3
Fe	12% C, 8% O	1.14	+10	2.1
Mo	15% C, 5% O	1.145	+5	1.3
Ni	12% C, 1% O	1	+12	1.1
Pt	24% C, 6% O	4	+12	0.4
Ti	14% C, 15% O	1.14	+5	0.2
V	15% C, 2% O	1	+5	0.7

RFA voltage from a few volts below V_S to a few volts above V_S, resulting in a retarding voltage V_{RET} which varied from a few volts below zero to a few volts above zero. Our measurement of the width of the energy-resolution function of the RFA, based on measurements of the Cu work function, provided an upper limit of 0.2 eV.

We define the pass energy of the positrons as

$$E_{\mathrm{pass}}=eV_{\mathrm{RET}}-\phi_g^-+\phi_S^- , \tag{4}$$

where $\phi_g^- - \phi_S^-$ is the electron contact potential difference between the RFA grid and the sample.[10] The energy associated with the motion of the positron in the z direction (normal to the surface) is defined as $E_Z \equiv \frac{1}{2}mv_z^2$. Positrons with $E_Z \geq E_{\mathrm{pass}}$ will be able to reach the detector. Positrons with $E_Z < E_{\mathrm{pass}}$ will return to annihilate at the sample. Neglecting the finite resolution of the RFA, the number of positrons that reach the MCP corresponds to the integral

$$I(E_{\mathrm{pass}})=\int_{E_{\mathrm{pass}}}^{\infty} N(E_z)dE_z , \tag{5}$$

where $N(E_Z)$ is the number of positrons per unit energy leaving the sample with energy E_Z. The distribution $N(E_Z)$ is equal to zero for $E_Z<0$ and is finite for $E_Z>0$. Therefore $I(E_{\mathrm{pass}})$ is constant for $E_{\mathrm{pass}}<0$ eV and starts to decrease at $E_{\mathrm{pass}}=0$ eV. The quantity measured in our experiment, $N(V_{\mathrm{RET}})$, is the number of detected positrons as a function of V_{RET} (see Fig. 2). It is related to $I(E_{\mathrm{pas}})$ by a constant factor corresponding to the detector efficiency and by a shift in the energy zero determined from Eq. (4). This shift is determined experimentally from the data by determining the value V_{zero} at which $N(V_{\mathrm{VET}})$ just begins to decrease (i.e., where $E_{\mathrm{pass}}=0$ eV).

Thermalized positrons can leave the surface with energies up to $-\phi^+$ in the z direction. Since most of the positrons are emitted normal to the surface,[11] the point of steepest descent in $N(V_{\mathrm{RET}})$ (the peak of the negative derivative) occurs at $V_{PK}=-\phi^+/e+V_{\mathrm{zero}}$. The curve does not drop completely to zero at that point because of "nonthermal" positrons, i.e., positrons that escape from the surface before reaching thermal equilibrium.[12]

The positron yield (the ratio of the number of positrons reemitted by the sample—for negative bias—to the incident flux) for each sample is included in Table I, along with surface contamination, incident positron energy, and voltage applied to the sample.

III. RESULTS AND DISCUSSION

Two methods were used to extract positron work functions from the data. In the first method, the work function, $\phi^+(1)$, is obtained by subtracting the value of the retarding voltage at the zero-energy point, V_{zero}, from the value at the point of steepest descent, V_{PK}.[14] The point of steepest descent is determined by differentiating $N(V_{\mathrm{RET}})$, which yields a well-defined peak. The value of V_{zero} is obtained by averaging points on the high shoulder ($E>0$) of the curve, and then determining the first

TABLE II. Positron work function results via two methods. ϕ^+ (1): from the difference $(V_{PK}-V_{\mathrm{RET(zero)}})$. $\phi^+(2)$: from the bulk chemical potential sums Σ as obtained from the peak positions V_{PK} referenced to Cu. All numbers are in eV.

Sample	eV_{PK}	$\phi^+(1)$ $=e(V_{PK}-V_{\mathrm{zero}})$	$\Delta\Sigma$ $=e(V_{PK}-V_{PK}^{\mathrm{Cu}})$	Σ $=\Sigma_{\mathrm{Cu}}+\Delta\Sigma$	ϕ^- [a]	$\phi^+(2)$ $=-\Sigma-\phi^-$
Cu	−0.2	−0.6	0	−4.3[b]	4.65	−0.4
Fe	0.8	−1.3	1.0	−3.3	4.5	−1.2
Mo	1.7	−2.4	1.9	−2.45	4.6	−2.2
Ni	0.1	−0.9	0.3	−4.0	5.15	−1.2
Pt	0.3	−1.5	0.5	−3.8	5.6	−1.8
Ti	—	>0	—	—	4.3	>0
V	0.4	−0.9	0.6	−3.7	4.3	−0.6

[a]Values taken from Ref. 24.

[b]The references values used here is given by Gidley and Frieze in Ref. 2, and it is in good agreement with earlier values in Refs. 8 and 19.

point lying at least 3 standard deviations below the average. A least-squares fit line is then drawn through this point and the two points on either side of it. The value of V_{RET} at the point of intersection of this line with the line representing the average of the high shoulder points is then taken as V_{zero} (see Fig. 2). There is a problem in determining work functions in this way. The analyzer's energy-resolution function shifts the determination of V_{zero} downward (to the left in Fig. 2), and the amount of shift depends on the functional form of the tails of the resolution function, which is not well known. To avoid problems with the measurement of V_{zero}, a second method to determine the work function, $\phi^+(2)$, (which will be discussed below) was used in which the energy spectrum for each sample was compared to that for Cu mounted in the spectrometer at the same time. The results of both methods of determining the work functions are given in Table II.

The energy spectra of reemitted positrons for the measured samples are shown in Figs. 2(a)–2(g). For each measurement, a plot was made of $N(V_{RET})$ as well as a curve representing the negative of a smoothed derivative[13] of $N(V_{RET})$. Both curves were normalized to unity. Note that the data for titanium [Fig. 2(f)] differs substantially in form from the data obtained from the other samples. Even though there is a point where $N(V_{RET})$ starts to go down, the data does not show a definite peak when differentiated. The integral curve, $N(V_{RET})$, seems to decrease exponentially to the right. Following Gullikson and Mills[15] [who had similar data for Al(111)], it is assumed that the observed spectrum is due to nonthermalized positrons. This leads to the conclusion that titanium has a positive positron work function.

As mentioned previously, different crystalline facets of the same material will have, in general, different work functions. Therefore, a polycrystalline sample would be expected to exhibit positron-work-function values which are characteristic of each crystal face present on the sample surface.[8] The area of the surface under the incident positron beam may consist of macroscopic patches of different faces, and each patch contributes to the local electric field. However, given sufficiently good statistics and ignoring resolution effects, measurements of $\phi^+(1)$ would yield the most negative value of ϕ^+ represented on the polycrystalline surface. The reason for this is as follows. The shoulder of $N(V_{RET})$ occurs at $V_{RET\,(zero)}$, the point at which E_{pass} equals zero. Setting $E_{pass}=0$ in Eq. (4) yields

TABLE III. Comparison of the positron work function values obtained in this experiment with theoretical and experimental values obtained elsewhere.

Sample	Surface	$\phi^+_{experiment}$ (eV)	ϕ^+_{theory} (eV)
Cu	poly	$-0.4(2)^*$	0.9[a], 0.8,[b] -1.0[c]
	(100)	>0[d]	$+0.22$[e]
	(100)+S	-1.2[f]	
	(110)	$-0.13(8)$[g]	$+0.33$[e]
	(110)+S	-0.4[g]	
	(111)	$-0.4(1)$[g], -0.33[f]	-0.13[e]
	(111)+S	-0.87[f], $-0.78(5)$[h]	
Fe	poly	$-1.2(2)^*$	-1.2,[a] -0.8[b]
Mo	poly	$-2.2(2)^*$, <0[i]	-1.6,[a] -2.0[b]
	(100)	-1.7[j]	-2.65[e]
	(100)+O	-2.7[j]	
	(110)		-3.03[e]
	(111)	<-3[d]	-2.67[e]
Ni	poly	$-1.2(2)^*$, <0[k]	-0.1,[a] -0.4[b]
	(100)	$-1.0(1)$,[k] $-1.3(1)$[l]	-0.77[e]
	(100)+O	-0.95[m]	
	(100)+CO($c2\times2$)	-1.6[m]	
	(100)+S($c2\times2$)	-1.6[m]	
	(110)	$-1.4(1)$[f]	-0.59[e]
	(111)		-0.90[e], -0.4[k]
Pt	poly	$-1.8(2)^*$	-0.2[b]
	(100)	$-1.9(1)$[k]	
	(100)+CO	$-2.2(1)$[k]	
Ti	poly	$>0^*$	-0.7,[a] $+0.1$[b]
V	poly	$-0.6(2)^*$	-0.4,[a] -1.7[b]

*This work.
[a]Reference 16.
[b]Reference 17.
[c]Reference 5.
[d]Reference 6.
[e]Reference 18.
[f]Reference 19.
[g]Reference 8.
[h]Reference 10.
[i]Reference 20.
[j]Reference 21.
[k]Reference 1.
[l]Reference 12.
[m]Reference 22.

$$eV_{\text{zero}} = \phi_g^- - \phi_s^- \ , \tag{6}$$

where, as before, the subscripts s and g refer to the sample and grid respectively. The point of steepest descent occurs at $E_{\text{pass}} = \phi^+$. Substitution of this value into Eq. (4) gives, along with Eqs. (1) and (2) and some rearrangement:

$$eV_{PK} - \phi_g^- = -\phi_S^- - \phi_S^+ = \mu^- + \mu^+ \ . \tag{7}$$

Since the chemical potential μ is a bulk property, so is the quantity,[23] $\mu^- + \mu^+ \equiv \Sigma$. This implies that if ϕ_g^- remains constant, then the position of the point of steepest descent is independent of the crystal face as well as surface contamination. Rather, the face dependence of the work function is reflected in the value of $V_{\text{RET (zero)}}$. Using the definition of Σ given above to rewrite Eq. (6) yields

$$eV_{\text{zero}} = \phi_g^- + \Sigma + \phi_S^+ \ . \tag{8}$$

If more than one face is present then the integral spectra will consist of a superposition of spectra from each face. Each component spectrum will show a decrease at the value of V_{zero} corresponding to that face. The first decrease in the superimposed spectra will occur at the value of V_{zero} for the crystal face with the most negative positron work function. In practice, counting statistics would make it difficult to determine V_{zero} for a crystal face which is not well represented on the sample surface. Surface contamination will also effect the position of eV_{zero}.

The second method used to determine the work function, $\phi^+(2)$, circumvents the problems associated with determining V_{zero}—surface contamination and the polycrystalline nature of the sample—by inferring the work function from a relative measurement of Σ that relied only on the values of V_{PK}. Since copper was mounted with the other samples for all of the measurements, the peak positions are referenced to copper. We define

$$\Delta\Sigma \equiv \Sigma - \Sigma_{\text{Cu}} = e(V_{PK} - V_{PK}^{\text{Cu}}) \ , \tag{9}$$

where the superscript Cu refers to the value for the Cu sample. Using the definition of Σ, Eq. (9) can be rearranged to give

$$\phi^+ = e(V_{PK}^{\text{Cu}} - V_{PK}) - \Sigma_{\text{Cu}} - \phi^- \ . \tag{10}$$

The values of $\phi^+(2)$ given in Table II were computed from our measurements using Eq. (10) along with a value of Σ_{Cu} obtained from Ref. 2 and values of ϕ^- for polycrystalline surfaces obtained from the compilation in Ref. 24. Values of ϕ^+ for specific single-crystal faces could also be inferred from our data by using Eq. (10) along with the value of ϕ^- corresponding to that crystallographic face.

TABLE IV. Comparison between experimental and theoretical values of $\Sigma = \mu^+ + \mu^-$. (The experimental values were determined from our data unless otherwise specified.)

Sample	$\Sigma_{\text{experiment}}$ (eV)	Σ_{theory} (eV)
Cu	-4.3[c]	-5.55,[a] -4.81[b]
Fe	-3.3	-3.3[a]
Mo	-2.4, -2.45[c]	-3.0,[a] -1.92[b]
Ni	-4.0, -3.8[c]	-5.05,[a] -4.46[b]
Pt	-3.8	—
Ti	—	-3.6[a]
V	-3.7	-3.9[a]

[a]Reference 16.
[b]Reference 18.
[c]Reference 12.

IV. CONCLUSIONS

We have obtained the positron work function values of polycrystalline Fe, Mo, Ni, Pt, and V, and have shown that polycrystalline Ti has a positive positron work function. The work functions of Fe, V, and Ti have not, to our knowledge, been previously published. Two methods were used to extract the work function. The first method provides an absolute measurement of the work function but suffers from systematic effects due to the spectrometer resolution function, the polycrystalline nature of the foil samples and surface contamination. The second method infers the positron work function from measurements of $\Sigma = \mu^+ + \mu^-$ relative to the value of Σ for Cu and values of the electron work function for the surface. The maximum difference between the two methods is 0.3 eV. While not giving an absolute measure of ϕ^+, the second method circumvents many of the systematic problems affecting the first method since the values of Σ are independent of crystal face and surface contamination. It should therefore be expected to give the relative values of ϕ^+ more accurately. Our results are in reasonable agreement with theoretical predictions for all samples studied except for Cu (Table III).

Our values for Σ (Table IV) are in reasonable agreement with theoretical predictions, and our Mo and Ni values agree very well with Gidley and Frieze's.

ACKNOWLEDGMENTS

We would like to acknowledge the technical assistance of D. Coyne, W. Lutes, and D. Miller. This work was supported, in part, by the Robert A. Welch Foundation, the Texas Advanced Technology Research Program, the Texas Advanced Research Program, and the Carver Scientific Research Initiative Grants at the University of Northern Iowa.

*Current address: General Dynamics, FW Division Fort Worth, Texas 76101.
†Current address: RSEG Group, Texas Instruments, Dallas, Texas 75070.

[1]P. J. Schultz and K. G. Lynn, Rev. Mod. Phys. **60**, 3 (1988).
[2]D. W. Gidley and W. E. Frieze, Phys. Rev. Lett. **60**, 1193 (1988).
[3]D. Mehl, A. R. Koymen, K. O. Jensen, F. Gotwald, and A.

Weiss, Phys. Rev. B **41**, 799 (1990).
[4]N. D. Lang and W. Kohn, Phys. Rev. B **3**, 1215 (1971).
[5]C. Hodges and M. Stott. Phys. Rev. B **7**, 73 (1973).
[6]A. P. Mills, Jr., in *Proceedings of the International School of Physics "Enrico Fermi" 1981,* edited by W. Brandt (North-Holland, New York, 1983), p. 432.
[7]C. Lei, D. Mehl, A. R. Koymen, K. O. Jensen, F. Gotwald, M. Jibaly, and A. Weiss, Rev. Sci. Instrum. **60**, 3656 (1989); M. Jibaly, D. Sc. Dissertation, The University of Texas at Arlington, 1987 (unpublished).
[8]C. A. Murray, A. P. Mills, Jr., and J. E. Rowe, Surf. Sci. **100**, 647 (1980).
[9]A. Stamatovic and G. J. Schulz, Rev. Sci. Instrum. **39**, 1752 (1968).
[10]C. A. Murray and A. P. Mills, Jr., Solid State Commun. **34**, 789 (1980).
[11]A. P. Mills, Jr., P. M. Platzman, and B. L. Brown, Phys. Rev. Lett. **41**, 1076 (1978).
[12]D. A. Fischer, K. G. Lynn, and W. E. Frieze, Phys. Rev. Lett. **50**, 1149 (1983); E. M. Gullikson, A. P. Mills, Jr., W. S. Crane, and B. L. Brown, Phys. Rev. B **32**, 5484 (1985).
[13]A. Savitzky and M. Golay, Anal. Chem. **36**, 1627 (1964).
[14]R. J. Wilson and A. P. Mills, Jr., Surf. Sci. **128**, 70 (1983).
[15]E. Gullikson and A. P. Mills, Jr., Phys. Rev. B **35**, 8759 (1987).
[16]G. Fletcher, J. L. Fry, and P. C. Pattnaik, Phys. Rev. B **27**, 3987 (1983).
[17]R. Nieminen and C. Hodges, Solid State Commun. **18**, 1115 (1976).
[18]O. V. Boev, M. J. Puska, and R. M. Nieminen, Phys. Rev. B **36**, 7786 (1987).
[19]D. A. Fischer, K. G. Lynn, and D. W. Gidley, Phys. Rev. B **33**, 4479 (1986).
[20]E. Gramsch, J. Throwe, and K. G. Lynn, Appl. Phys. Lett. **51**, 1862 (1987).
[21]B. Nielsen, K. G. Lynn, A. Vehanen, and P. J. Schultz, Phys. Rev. B **32**, 2296 (1985).
[22]D. A. Fischer, Ph.D. dissertation, SUNY, Stony Brook, 1984. Available from University Microfilms International (No. 85-13537).
[23]W. E. Frieze, D. W. Gidley, and B. D. Wissman, Solid State Commun. **74**, 1079 (1990).
[24]J. Holzl, *Solid Surface Physics,* Springer Tracts in Modern Physics 85 (Springer-Verlag, New York, 1979), p. 85.